Eur. Phys. J. A **46**, 337–343 (2010)
DOI 10.1140/epja/i2010-11058-1

THE EUROPEAN PHYSICAL JOURNAL A

Regular Article – Experimental Physics

The new isotope ^{208}Th

J.A. Heredia[1,2,a], A.N. Andreyev[3,4,5], S. Antalic[6], S. Hofmann[2,7], D. Ackermann[2], V.F. Comas[1,2], S. Heinz[2], F.P. Heßberger[2], B. Kindler[2], J. Khuyagbaatar[2], B. Lommel[2], and R. Mann[2]

[1] FIAS, Goethe-Universität Frankfurt, 60438 Frankfurt, Germany
[2] GSI Helmholtzzentrum für Schwerionenforschung (GSI), 64291 Darmstadt, Germany
[3] School of Engineering and Science, University of the West of Scotland, Paisley, PA1 2BE, UK
[4] The Scottish Universities Physics Alliance (SUPA), UK
[5] Instituut voor Kern- en Stralingsfysica, K.U. Leuven, University of Leuven, 3001 Leuven, Belgium
[6] Department of Nuclear Physics and Biophysics, Comenius University, 84248 Bratislava, Slovakia
[7] Institut für Physik, Goethe-Universität Frankfurt, 60054 Frankfurt, Germany

Received: 16 July 2010 / Revised: 14 October 2010
Published online: 9 November 2010 –
Communicated by N. Alamanos

Abstract. The new neutron-deficient isotope ^{208}Th was produced in the complete-fusion reaction $^{64}\mathrm{Ni} + {}^{147}\mathrm{Sm} \rightarrow {}^{208}\mathrm{Th} + 3\mathrm{n}$. Evaporation residues were separated in-flight by the velocity filter SHIP and subsequently identified on the basis of energy-, position- and time-correlated α-decay chains. The measured α-decay energy and half-life value of ^{208}Th are 8044(30) keV and $1.7^{+1.7}_{-0.6}$ ms, respectively. Improved data on the α-decay of ^{209}Th, ^{210}Th, ^{212}Th and ^{208}Ra were obtained using complete-fusion reactions of ^{64}Ni with ^{147}Sm, ^{150}Sm, and ^{152}Sm targets.

1 Introduction

Alpha-decay studies are often the only method to obtain spectroscopic and mass information on the heavy nuclei close to the proton drip line. Since long, the most efficient method of producing these nuclei has been heavy-ion–induced complete-fusion reactions followed by neutron evaporation, until recently the promising application of the projectile fragmentation method at FRS (GSI) to produce neutron-deficient Fr-Th nuclei was demonstrated [1,2].

The goal of the present work was to obtain improved data for the most neutron-deficient isotopes of thorium with masses $A \leq 212$, whose decay properties were poorly known. Furthermore, according to calculations (*e.g.*, [3]) an onset of deformation is expected from ^{212}Th on, with an oblate deformation of $\beta_2 = -0.182$ predicted for ^{208}Th. This effect could possibly be seen in the decay properties of the lightest Th isotopes, studied in this work. In the past, several experiments had been performed to study the nuclei in this region: ^{212}Th was investigated in [4] (18 decay events were measured), ^{211,210}Th in [5] (2 decay chains for ^{210}Th) and ^{209}Th in [6] (2 decay chains).

In our work, we identified the new isotope ^{208}Th and obtained improved data for the isotopes ^{209,210,212}Th.

[a] e-mail: j.heredia@gsi.de

2 Experimental setup

In our study, the neutron-deficient isotopes of thorium were produced in complete-fusion reactions of ^{64}Ni ions with different enriched Sm targets. The relevant beam energies and targets used are given in table 1.

A pulsed ^{64}Ni beam (5 ms beam on/15 ms beam off) with a typical intensity of 500 pnA was provided by the UNILAC of the GSI (Darmstadt, Germany). Eight target segments of a specific Sm isotope were mounted on a target wheel rotating synchronously with the UNILAC macropulsing.

The targets were prepared from isotopically enriched material of $^{152}SmF_3$, $^{150}SmF_3$ and $^{147}SmF_3$ with an enrichment of 98.4%, 95.6% and 96.4%, respectively. Samarium fluoride layers with a thickness in the range of 327–546 μg/cm^2 were evaporated on carbon foils of 40 μg/cm^2 and covered with a layer of 10 μg/cm^2 of carbon in order to improve the radiative cooling and to reduce material losses by sputtering [7].

After separation by the velocity filter SHIP [8] the evaporation residues (ERs) were implanted into a 300 μm thick, 35 × 80 mm^2 16-strip position-sensitive silicon detector (PSSD) mounted at the focal plane of SHIP [9], where their subsequent particle decays were measured. The α-energy calibration of the PSSD was performed by using the known α-lines of the isotopes $^{197-200}$Po, ^{204}Rn, ^{208}Ra, and ^{211}Ac that all have an uncertainty of

Table 1. Beam energies E_{lab} at the beginning of the target, number of observed correlated events N and production cross-sections σ.

Isotope	Reaction	E_{lab}/MeV	N	σ/pb
^{212}Th	^{64}Ni + ^{152}Sm $\rightarrow^{212}$ Th + 4n	288	1430	34000(900)
^{210}Th	^{64}Ni + ^{150}Sm $\rightarrow^{210}$ Th + 4n	294	165	1590(130)
^{209}Th	^{64}Ni + ^{147}Sm $\rightarrow$ ^{209}Th + 2n	288	4	29^{+22}_{-15}
^{208}Th	^{64}Ni + ^{147}Sm $\rightarrow$ ^{208}Th + 3n	288	3	22^{+20}_{-13}
	^{64}Ni + ^{147}Sm $\rightarrow$ ^{208}Th + 3n	294	1	95^{+219}_{-79}

~ 5 keV [10]. These isotopes were produced either directly in different evaporation channels of the studied reactions or were the decay products of directly produced nuclei. The broad energy range of $\sim$ 5800–7500 keV and a small energy uncertainty for the majority of the α-lines used for the calibration allowed us to make a reliable calibration extrapolation into the α-energy region of 7800–8200 keV, relevant for the Th isotopes studied in our work. A typical α-energy resolution of each strip of the PSSD was $\sim$ 25 keV (FWHM) in the energy interval 6000–8200 keV. Since α emission is the dominant decay mode of most of the nuclei produced in the considered reactions, the identification of nuclides was based on the observation of genetically correlated α-decay chains.

Upstream the PSSD, six silicon detectors of similar shape (box detectors) were mounted in an open box geometry; see [11] for details. They were used to measure the energies of α-particles escaping from the PSSD in the backward direction. By adding up the energy deposition in the PSSD and box detectors, the full energy of the escaping α-particles could be recovered, though with a somewhat reduced energy resolution. A typical α-energy resolution for the sum signal was $\sim$ 70 keV (FWHM), which was in most cases sufficient to unambiguously distinguish the decays of interest.

Together with the box+PSSD system in front of which they were placed, three time-of-flight detectors (TOF) [12] allowed us to distinguish the reaction products from the scattered beam particles, transfer reaction products and scattered target-like nuclei. More importantly, decay events in the PSSD could be distinguished from the implantation events by requiring an anticoincidence condition between the signals from the PSSD and from at least one of the TOF detectors.

Behind the PSSD a fourfold segmented Clover detector was installed for prompt and delayed α–γ or α–X-ray coincidence measurements within a time window of $\Delta T(\alpha\text{-}\gamma) \leq 5\,\mu$s.

3 Experimental results

Two beam energies of 288(1) and 294(1) MeV at the beginning of the target were used in our experiments (see table 1). These energies correspond to the expected maxima of production cross-sections of fusion evaporation channels of our interest, as calculated with the HIVAP statistical model code [13].

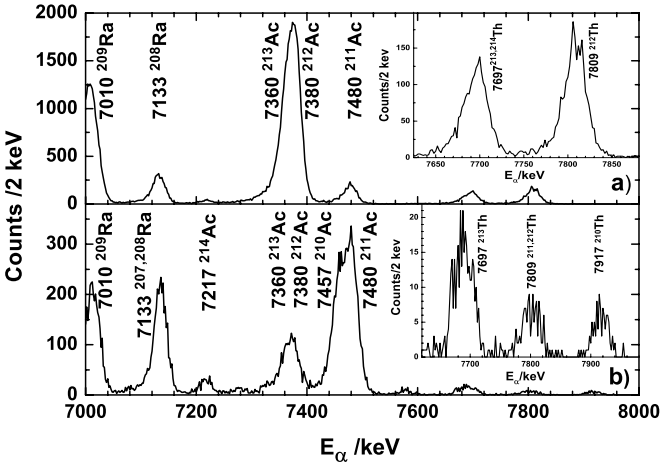

Fig. 1. Energy spectra of the α-decays in the PSSD, collected between the beam pulses in the reactions ^{64}Ni(288 MeV) + ^{152}Sm $\rightarrow$ ^{212}Th + 4n (a) and ^{64}Ni(294 MeV) + ^{150}Sm $\rightarrow^{210}$ Th + 4n (b). Some peaks are labeled with the α-decay energy (in keV) and the isotope to which the α-decay belongs. In the broader double peaks of ^{210,211}Ac, ^{212,213}Ac, ^{207,208}Ra, ^{211,212}Th and ^{213,214}Th we just included earlier reported literature values to guide the reader.

The errors of the half-life values and production cross-sections were determined by the procedure described in [14].

No α-γ coincidences were seen for the discussed α-decays.

3.1 ^{210}Th and ^{212}Th isotopes

The energy spectra of α-decays, measured in the PSSD in pauses between beam pulses ("beam off" time interval) for the reactions ^{64}Ni(288 MeV) + ^{152}Sm $\rightarrow$ ^{212}Th + 4n and ^{64}Ni(294 MeV) + ^{150}Sm $\rightarrow$ ^{210}Th + 4n are shown in figs. 1a and b, respectively. The main peaks in the spectra are due to α-decays of the ^{210,211,212,213,214}Ac and ^{207,208,209}Ra isotopes produced by pxn and αxn evaporation channels, respectively, whereas the Th isotopes were all produced by xn channels. Several pairs of isotopes in this region have quite similar energies (^{210,211}Ac,

Table 2. α-particle energies, half-lives and reduced α-widths of parent activities measured in the present work and compared with earlier measurements. The half-lives calculated with the semi-empirical formula found in [22] are given in the last column.

Nuclei	E_α/keV	$T_{1/2}$/ms	δ^2_α/keV	E_α/keV	$T_{1/2}$/ms	Ref.	$T_{1/2}$/ms (from [22])
	Present work			Literature			
^{212}Th	7809(5)	31.7(1.3)	56(3)	7802(10)	30^{+20}_{-10}	[4]	10
^{210}Th	7917(6)	16.0(3.6)	55(13)	7899(17)	9^{+17}_{-4}	[5]	4.6
^{209}Th	8123(25)	$2.5^{+1.7\,a}_{-0.7}$	87^{+61}_{-29}	8080(50)	$3.8^{+6.9}_{-1.5}$	[6]	3.5
^{208}Th	8044(30)	$1.7^{+1.7}_{-0.6}$	229^{+234}_{-94}	–	–	–	1.9

[a] Including the 2 events from [6]. With our 4 events only: $T_{1/2} = 1.9^{+1.9}_{-0.7}$ ms (see table 3 and sect. 3.2).

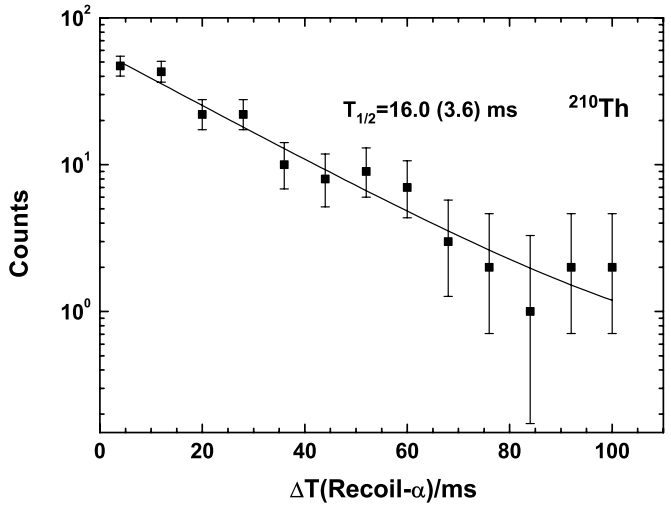

Fig. 2. ER-α time distribution of the ^{210}Th α-decays from fig. 1b. The continuous solid line shows the result of an exponential decay fit.

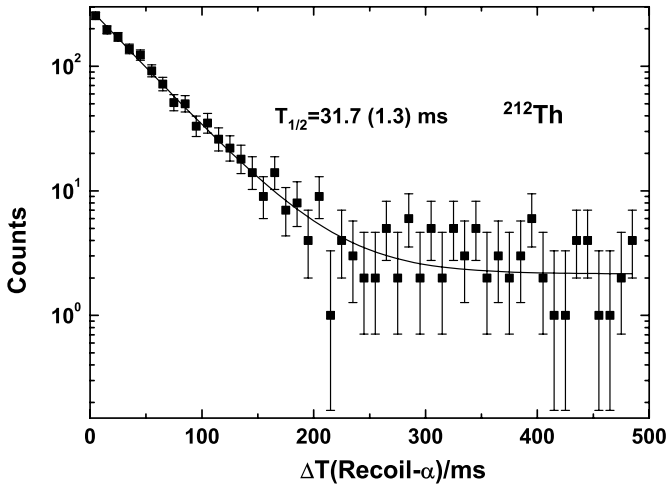

Fig. 3. ER-α time distribution of the ^{212}Th α-decays from fig. 1a. The continuous solid line shows the result of an exponential decay fit with a constant background.

^{212,213}Ac, ^{207,208}Ra, ^{211,212}Th and ^{213,214}Th), which could lead to two α-decays combined in one broader peak. However, in most cases, due to the proper choice of the beam energy, only one of the isotopes within each pair was dominantly produced, while the contribution of the second decay was usually negligible (see also below). The presence of ^{213}Th and ^{213,214}Ac in fig. 1b is explained by a small admixture of the heavier ^{152,154}Sm isotopes in the ^{150}Sm target, as these Th and Ac isotopes are not expected to be produced at this beam energy on the ^{150}Sm target.

The ERs-α correlation analysis was performed for known α-decays of ^{212}Th and ^{210}Th in the α-energy intervals of $E_\alpha(^{212}\text{Th}) = (7.76\text{–}7.86)$ MeV and $E_\alpha(^{210}\text{Th}) = (7.87\text{–}7.97)$ MeV, respectively. ER-α time windows of 500 ms and 120 ms were used for ^{212}Th and ^{210}Th, respectively. In total, 1430 (^{212}Th) and 165 (^{210}Th) correlated ER-α chains were found. From the respective time distributions between the recoil implantation and subsequent α-decays more precise half-life values of 16.0(3.6) ms for ^{210}Th and 31.7(1.3) ms for ^{212}Th were deduced (fig. 2 and fig. 3). Improved α-decay energy values for these isotopes were also obtained: $E_\alpha(^{210}\text{Th}) = 7917(6)$ keV and $E_\alpha(^{212}\text{Th}) = 7809(5)$ keV (table 2). The measured cross-sections are given in table 1.

A possible contribution of α-decays of ^{211}Th, which could be weakly produced in the 5n evaporation channel of the $^{64}\text{Ni} + {}^{152}\text{Sm} \rightarrow {}^{216}\text{Th}^*$ reaction, to the α-decay peak of ^{212}Th had to be carefully considered in fig. 1a. This is because the reported α-decay energy (7.792(14) MeV) and half-life value (37^{+28}_{-11} ms) of ^{211}Th [5] are comparable to those of ^{212}Th, thus based on decay properties alone their clear separation is not possible. However, with the proper choice of the beam energy in our study, which corresponded to the dominant evaporation channels with four nucleons (^{212}Ac and ^{212}Th), the contribution of ^{211}Th (5n channel) is small. This is confirmed by the comparison of the intensities of the ^{212}Ac (p3n channel) and of ^{211}Ac (p4n channel) in fig. 1a, which shows that the production of the channel with evaporation of five nucleons was indeed lower by a factor of ten at the beam energy of 288 MeV.

A correlation analysis of the type α_1-α_2 with an 8 s time window was performed for ^{212}Th-^{208}Ra chains. Based on this analysis, a half-life value of 1110(45) ms was deduced for ^{208}Ra (fig. 4) and an α branching ratio of 87(3)% was derived for the first time. The previous reported values for the half-life and for the EC/β^+ branching (based on systematics) were of 1.3(2) s and 5% [15], respectively.

Table 3. Energies deposited in the stop detector (or sum energies from stop and box detectors) and time intervals between ER-α_1 and α_x-α_{x+1} for our ^{208}Th and ^{209}Th decay chains. Mean α-particle energies and partial α-decay half-lives of parent activities measured in the present chains and compared with earlier measurements are given.

Event no.	^{209}Th		^{205m}Ra		^{201m}Rn		^{197m}Po	
	E_{α_1}/keV	Δt/ms	E_{α_2}/keV	Δt/ms	E_{α_3}/keV	Δt/s	E_{α_4}/keV	Δt/s
1	8099	4.2	7392	124	6728[b]	11.3	6379	28.67
2	8135	1.7	7366	92.4	6758[b]	2.98	–	–
3	8136	1.1	7365[b]	64.9	6787	0.767	–	–
4	8136[b]	4.0	7392[b]	112	3779[a]	3.65	6389	13.01
		$T_{1/2}$/ms		$T_{1/2}$/ms		$T_{1/2}$/s		$T_{1/2}$/s
1+2+3+4[c]	8123(25)	$1.9^{+1.9}_{-0.7}$	7379(30)	68^{+68}_{-23}	6787(30)	$3.24^{+3.24}_{-1.08}$	6384(30)	$14.45^{+14.45}_{-4.9}$
Lit.	8080(50) [6]	$3.8^{+6.9}_{-1.5}$ [6]	7370(20) [10,16,17]	170^{+60}_{-40} [15]	6772(3) [10]	3.8(1) [15]	6383(3) [10]	30.7(1) [15]

	^{208}Th		^{204}Ra		^{200}Rn		^{196}Po	
	E_{α_1}/keV	Δt/ms	E_{α_2}/keV	Δt/ms	E_{α_3}/keV	Δt/s	E_{α_4}/keV	Δt/s
5	8018	6.1	7485	58.6	6849[b]	0.980	–	–
6	8070	0.7	7481	38.0	547[a]	6.65	6536[b]	9.68
7	7975[b]	1.9	7495	24.1	6914	0.571	6522	5.00
8	7893[b]	0.9	7475	132	1644[a]	0.064	6522	3.05
		$T_{1/2}$/ms		$T_{1/2}$/ms		$T_{1/2}$/s		$T_{1/2}$/s
5+6+7+8[c]	8044(30)	$1.7^{+1.7}_{-0.6}$	7484(25)	44^{+44}_{-15}	6914(30)	$1.4^{+1.4}_{-0.5}$	6522(25)	$4.1^{+5.6}_{-1.5}$
Lit.	–	–	7486(8) [10,16,17]	59^{+12}_{-9} [15]	6902(3) [10]	1.03(5) [15]	6521(3) [10]	6.17(20) [15]

[a] Escaped alpha, measured only in the PSSD, no coincident signal in the box detectors was observed.
[b] Decay energy is reconstructed by adding up the energy deposition in the PSSD and in the box detectors.
[c] Escaped ([a]) and reconstructed ([b]) events were only considered for the half-life calculations due to their worse energy resolution.

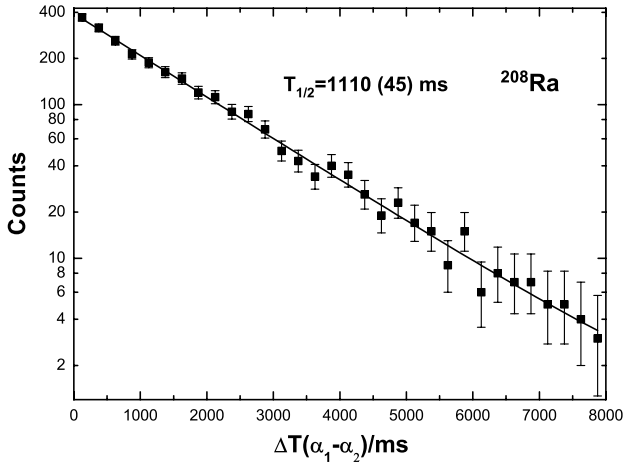

Fig. 4. α_1-α_2 time distribution of the ^{212}Th-^{208}Ra α-decays. The continuous solid line shows the result of an exponential decay fit.

3.2 ^{209}Th isotope

In a previous study, only two ^{209}Th α-decay events were reported, from which an energy of 8080(50) keV and a half-life value of $3.8^{+6.9}_{-1.5}$ ms were determined [6].

We produced the isotope ^{209}Th in the reaction ^{64}Ni + ^{147}Sm $\rightarrow$ ^{209}Th + 2n, see table 1. To achieve an unambiguous identification of ^{209}Th, produced with a rather low cross-section value, we searched for decay chains consisting of four consecutive α-decays, starting from the recoil implantation in the PSSD (ER-α_1(^{209}Th)-α_2(^{205}Ra)-α_3(^{201}Rn)-α_4(^{197}Po) correlation analysis).

A time window of Δ(ER-α) $\leq$ 20 ms and an energy interval of E_{α_1} = 7.8–8.3 MeV were used to search for the α-decays of ^{209}Th. To find the subsequent members of the correlation chains, time windows and energy intervals corresponding to the decay properties of the descendants of ^{209}Th, *i.e.* the isotopes ^{205}Ra, ^{201}Rn and ^{197}Po were used, which are shown in table 3. In our search for long-lived isotopes such as ^{197m}Po in our correlated decay chains we had to evaluate the probability of a chance coincidence. The probabilities of occurrence of such an event with an energy in the 6335–6415 keV interval (^{197m}Po) due to the alpha decay of two different evaporation residues (implanted at the same position) within 30 s, 60 s and 90 s are of only 4.3%, 8.3% and 12.3%, respectively. Four chains were assigned to the decay of the ^{209}Th isotope (table 3).

Based on these events, a decay energy of 8123(25) keV and a half-life of $1.9^{+1.9}_{-0.7}$ ms were deduced, which agree

with previously reported values [6] but are more precise, see table 2.

It is important to note here that within the limited accuracy of ±30 keV, the energies of the α_2–α_4 members of the observed decay chains of ^{209}Th are consistent with the reported α-decay energies of ^{205m}Ra (7370(20) keV [10, 16,17]), ^{201m}Rn (6772(3) keV [10]) and ^{197m}Po [10], rather than with the α-decay energies of ^{205g}Ra (7344(50) keV [10,16,17]), ^{201g}Rn (6723(50) keV [10]) and ^{197g}Po [10]. In particular, the deduced α-decay energy of ^{197}Po in our experiment (6384(30) keV) is in agreement with the tabulated value of 6383(3) keV for ^{197m}Po, rather than with the tabulated value of 6282(4) keV for ^{197g}Po. This suggests that the observed decays chains of ^{209}Th are of the type ER-α_1(^{209}Th)-α_2(^{205m}Ra)-α_3(^{201m}Rn)-α_4(^{197m}Po). This is in agreement with the previous study [6] who also observed ^{197m}Po as α_4-decay in the two chains measured (see sect. 4 for more details).

By using both the four decay time intervals ΔT(ER-α_1) from our study and the two reported time intervals ΔT(ER-α_1) for ^{209}Th from [6], we deduced the half-life value of $2.5^{+1.7}_{-0.7}$ ms for this isotope, provided in table 2. Due to an inferior α-energy resolution of 98 keV (FWHM) for the 6.779 MeV α-particles in [6], we could not use those two events to deduce the α-decay energy of ^{209}Th based on all six events.

3.3 The new isotope ^{208}Th

The new isotope ^{208}Th isotope was produced at two beam energies in the reaction ^{64}Ni + ^{147}Sm → ^{208}Th + 3n, see table 1. Similarly to ^{209}Th, a search for decay chains with four consecutive α-decays, starting from the recoil implantation in the PSSD was performed.

Four decay chains, shown in table 3, were found. The decay properties of the last three members of these chains are in good agreement with the published values of the descendants of ^{208}Th, *i.e.* the isotopes ^{204}Ra, ^{200}Rn and ^{196}Po. An α-decay energy of 8044(30) keV and a half-life of $1.7^{+1.7}_{-0.6}$ ms were deduced for ^{208}Th. The energy was deduced based on only the two events with the full energy deposition of the α_1-decay in the PSSD. For half-life determination, all four events were used.

4 Discussion

As mentioned above, our data indicate that the observed α-decays of ^{209}Th feed, most probably, the isomeric state in ^{205}Ra. This isomeric state has a tentative spin-parity assignment of $I^\pi = (13/2^+)$, based on systematics in neighboring odd-A nuclei and on the unhindered α-decay into the presumable $I^\pi = (13/2^+)$ isomer in ^{201}Rn [18,19].

The reduced α-decay width of $\delta^2_\alpha(^{209}\text{Th}) = 87^{+61}_{-29}$ keV can be deduced for the 8123(25) keV decay using the Rasmussen approach for $\Delta L = 0$ transitions [20]. This value is comparable to the reduced α-width of 55(13) keV for the neighboring isotope ^{210}Th, which suggests that the

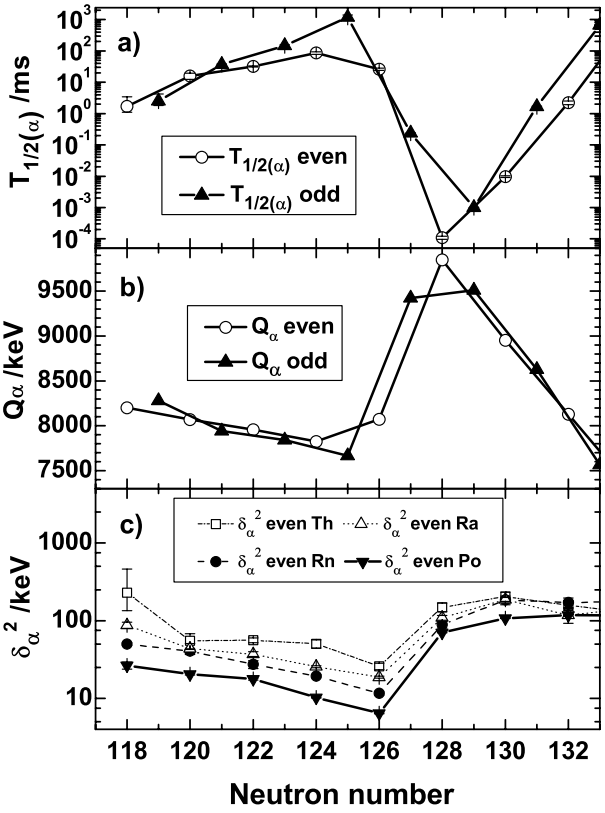

Fig. 5. α-decay systematics for the $118 \leq N \leq 132$ Th isotopes: (a) partial $T_{1/2(\alpha)}$ values; (b) Q_α-decay energies. For ^{209}Th, the value could be that of an isomeric state; (c) reduced α-widths for the even Th, Ra, Rn and Po isotopes.

8123 keV decay of ^{209}Th is unhindered and connects states with the same spin and parity in the parent ^{209}Th and daughter ^{205}Ra nuclei. Therefore, based on the tentative spin-parity assignment of $I^\pi = (13/2^+)$ for ^{205m}Ra, a tentative spin-parity assignment of $I^\pi = (13/2^+)$ could also be done for the state in ^{209}Th that decays by emission of 8123 keV α-particles.

This inference would also be in agreement with the well-known fact that in the complete-fusion reactions with heavy ions, the high-spin states have a preferential population in comparison with the low-spin states. Despite this, based on our data alone we cannot draw any definitive conclusion with regard to whether the observed state in ^{209}Th is the ground or excited state. However, it is known for lighter even-Z nuclei (Ra, Rn, Po) that the excitation energy of the $13/2^+$ states decreases gradually with decreasing neutron number. Since $13/2^+$ was assigned to an isomeric state at 1118 keV in ^{213}Th [21] and for lighter even-Z nuclei (Ra, Rn, Po) the decrease of the excitation energy of the $13/2^+$ states from $N = 123$ to $N = 119$ is lower than 730 keV, it is rather unlikely that the $I = 13/2^+$ state would become the ground state in ^{209}Th.

As can be seen from figs. 5a and b, our $T_{1/2(\alpha)}$ and Q_α values for ^{209}Th extend smoothly the respective systematics for the Th isotopes. However, the $Q_\alpha(^{208}\text{Th})$

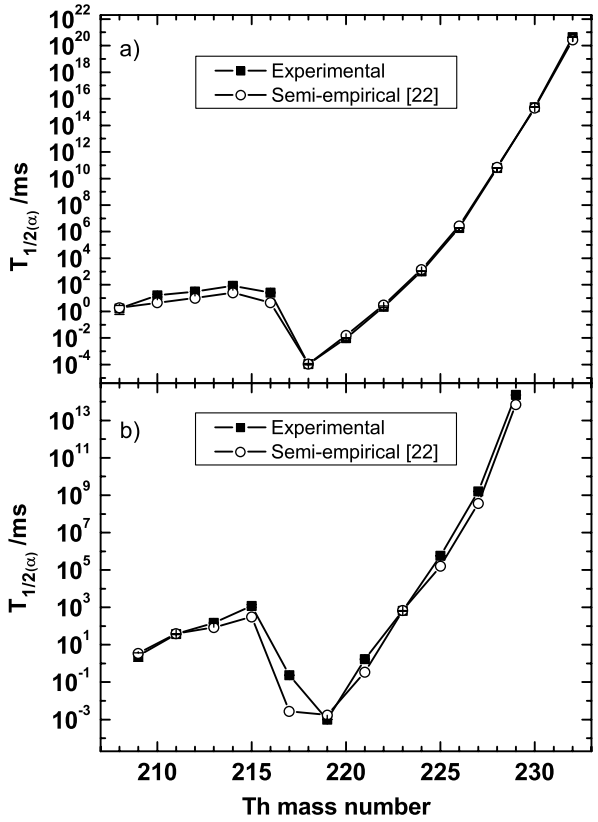

Fig. 6. Experimental and semi-empirically calculated [22] partial $T_{1/2(\alpha)}$ values for the even $^{208-232}$Th (a) and odd $^{209-229}$Th (b) isotopes.

value is slightly lower than that for ^{209}Th, and thus, does not follow this trend. This could possibly be explained as due to the above-proposed scenario of the decay from the $I = 13/2^+$ isomer in ^{209}Th. Another tentative scenario which could be suggested here is the influence of the (predicted) deformation (ref. [3]) setting in the lightest Th isotopes, from ^{212}Th on. However, we prefer not to draw any definitive inference in this case.

The systematics of reduced widths (δ^2_α) for even-even Po, Rn, Ra and Th isotopes with $118 \leq N \leq 132$ is shown in fig. 5c. Their comparison in this region of neutron numbers shows the smooth increase of values with the increase of atomic number (at the same neutron number). This is a feature generally accepted for the alpha-decay process. Note also the kink at $N = 126$ in reduced widths of all these elements, which is due to the neutron shell closure.

The reduced α-decay width of $\delta^2_\alpha(^{208}\mathrm{Th}) = 229^{+234}_{-94}$ keV was deduced for the 8044(30) keV decay using the Rasmussen approach for $\Delta L = 0$ transitions [20]. Within its large uncertainty, this value continues the smoothly increasing trend of the reduced α-widths of the even-even isotopes $^{210-216}$Th.

Calculations using the phenomenological formula found in [22] reproduce the α-decay half-life values fairly well, both for even-A $^{208-232}$Th and odd-A $^{209-229}$Th isotopes, see fig. 6. The calculated values for ^{208,209,210,212}Th isotopes are also given in table 2.

5 Conclusion

The new isotope ^{208}Th has been unambiguously identified by observing four decay chains leading to its known daughter products. The measured α-particle energy and half-life value are 8044(30) keV and $1.7^{+1.7}_{-0.6}$ ms, respectively.

Due to the observation of four α-decay chains, improved data on the α-decay of ^{209}Th has been obtained, namely, $T_{1/2} = 2.5^{+1.7}_{-0.7}$ ms and $E_\alpha = 8123(25)$ keV. Irradiation with other Sm targets allowed us to improve the known α-decay properties of ^{210}Th and ^{212}Th concerning energies ($E_\alpha(^{210}\mathrm{Th}) = 7917(6)$ keV and $E_\alpha(^{212}\mathrm{Th}) = 7809(5)$ keV) and half-lives ($T_{1/2}(^{210}\mathrm{Th}) = 16.0(3.6)$ ms and $T_{1/2}(^{212}\mathrm{Th}) = 31.7(1.3)$ ms), respectively.

It seems very interesting to continue studies of even lighter Th isotopes such as ^{207}Th and ^{206}Th to see if they follow the thorium systematics (fig. 5) although even smaller production cross-sections are expected. In fact, the very fast decrease of production cross-section values with decreasing neutron number made it very difficult to obtain significant statistics on the lighter Th isotopes produced in this work. Therefore, experiments with a higher beam dose are necessary to further investigate the properties of the lightest Th isotopes. In this respect, the use of fragmentation reactions could be another way to reach this region of nuclei [1,2].

We would like to express our gratitude to H.G. Burkhard and J. Maurer for their skillful maintenance of the mechanical and electrical components of SHIP. We thank the UNILAC staff as well as the ion source crew for delivering beams of high and stable intensity. We are also grateful to the GSI target lab for the production and preparation of the target wheels. S. Antalic, was supported by the Slovak grant agency VEGA (Contract No. 1/0091/10).

References

1. J. Kurcewicz, Z. Liu, M. Pfützner, P.J. Woods, C. Mazzocchi, K.-H. Schmidt, A. Kelić, F. Attallah, E. Badura, C.N. Davids, T. Davinson, J. Döring, H. Geissel, M. Górska, R. Grzywacz, M. Hellström, Z. Janas, M. Karny, A. Korgul, I. Mukha, C. Plettner, A. Robinson, E. Roeckl, K. Rykaczewski, K. Schmidt, D. Seweryniak, K. Sümmerer, H. Weick, Nucl. Phys. A **767**, 1 (2006).
2. Z. Liu, J. Kurcewicz, P.J.Woods, C. Mazzocchi, F. Attallah, E. Badura, C.J. Davids, T. Davinson, J. Döring, H. Geissel, M. Górska, R. Grzywacz, M. Hellström, Z. Janas, M. Karny, A. Korgul, I. Mukha, M. Pfützner, C. Plettner, A. Robinson, E. Roeckl, K. Rykaczewski, K. Schmidt, D. Seweryniak, H. Weick, Nucl. Instrum. Methods Phys. Res. A **543**, 591 (2005).
3. P. Möller, J.R. Nix, W.D. Myers, W.J. Swiatecki, At. Data Nucl. Data Tables **59**, 185 (1995).
4. D. Vermeulen, H.G. Clerc, W. Lang, K.H. Schmidt, G. Münzenberg, Z. Phys. A **294**, 149 (1980).
5. J. Uusitalo, T. Enqvist, M. Leino, W.H. Trzaska, K. Eskola, P. Armsbruster, V. Ninov, Phys. Rev. C **52**, 113 (1995).

6. H. Ikezoe, T. Ikuta, S. Hamada, Y. Nagame, I. Nishinaka, K. Tsukada, Y. Oura, T. Ohtsuki, Phys. Rev. C **54**, 2043 (1996).
7. B. Kindler, D. Ackermann, W. Hartmann, F.P. Heßberger, S. Hofmann, B. Lommel, R. Mann, J. Steiner, Nucl. Instrum. Methods Phys. Res. A **561**, 107 (2006).
8. G. Münzenberg, W. Faust, S. Hofmann, P. Armbruster, K. Güttner, H. Ewald, Nucl. Instrum. Methods **161**, 65 (1979).
9. S. Hofmann, G. Münzenberg, Rev. Mod. Phys. **72**, 733 (2000).
10. A.H. Wapstra, G. Audi, C. Thibault, Nucl. Phys. A **729**, 129 (2003).
11. A.N. Andreyev, D. Ackermann, F.P. Heßberger, S. Hofmann, M. Huyse, G. Münzenberg, R.D. Page, K. Van de Vel, P. Van Duppen, Nucl. Instrum. Methods Phys. Res. A **533**, 409 (2004).
12. S. Saro, R. Janik, S. Hofmann, H. Folger, F.P. Heßberger, V. Ninov, H.J. Schött, A.P. Kabachenko, A.G. Popeko, A.V. Yeremin, Nucl. Instrum. Methods Phys. Res. A **381**, 520 (1996).
13. W. Reisdorf, Z. Phys. A **300**, 227 (1981).
14. K.H. Schmidt, C.C. Sahm, K. Pielenz, H.G. Clerc, Z. Phys. A **316**, 19 (1984).
15. G. Audi, O. Bersillon, J. Blachot, A.H. Wapstra, Nucl. Phys. A **729**, 3 (2003).
16. M. Leino, J. Äystö, T. Enqvist, A. Jokinen, M. Nurmia, A. Ostrowski, W. H. Trzaska, J. Uusitalo, K. Eskola, P. Armbruster, V. Ninov, Acta Phys. Pol. B **26**, 309 (1995).
17. M. Leino, J. Uusitalo, R. G. Allatt, P. Armbruster, T. Enqvist, K. Eskola, S. Hofmann, S. Hurskanen, A. Jokinen, V. Ninov, R.D. Page, W.H. Trzaska, Z. Phys. A **355**, 157 (1996).
18. K. Andgren, B. Cederwall, J. Uusitalo, A.N. Andreyev, S.J. Freeman, P. T. Greenlees, B. Hadinia, U. Jakobsson, A. Johnson, P.M. Jones, D.T. Joss, S. Juutinen, R. Julin, S. Ketelhut, A. Khaplanov, M. Leino, M. Nyman, R.D. Page, P. Rahkila, M. Sandzelius, P. Sapple, J. Sarén, C. Scholey, J. Simpson, J. Sorri, J. Thomson, R. Wyss, Phys. Rev. C **77**, 054303 (2008).
19. F.G. Kondev, Nucl. Data Sheets **108**, 365 (2007).
20. J.O. Rasmussen, Phys. Rev. **115**, 1675 (1959).
21. J. Khuyagbaatar, S. Hofmann, F.P. Heßberger, D. Ackermann, S. Antalic, H.G. Burkhard, S. Heinz, B. Kindler, A.F. Lisetskiy, B. Lommel, R. Mann, K. Nishio, H.J. Schött, B. Sulignano, Eur. Phys. J. A **34**, 355 (2007).
22. A. Parkhomenko, A. Sobiczewski, Acta Phys. Pol. B **36**, 3095 (2005).